Gradient Selected Pure-Shift EASY-ROESY techniques facilitate the quantitative measurement of ^{1}H,^{1}H-distance restraints in congested spectral regions

Julian Ilgen[1], Jens Nowag[1], Lukas Kaltschnee[2,3], Volker Schmidts[1] and Christina M. Thiele[1]

1: Clemens-Schöpf-Institut für Organische Chemie und Biochemie, Technische Universität Darmstadt, Alarich-Weiss-Straße 16, D-64287 Darmstadt, Germany, cthiele@thielelab.de

2: Max-Planck-Institut für Biophysikalische Chemie, Am Fassberg 11, 37077 Göttingen, Germany

3: Center for Biostructural Imaging of Neurodegeneration (BIN), Von-Siebold-Str.3A,

37075 Göttingen, Germany

1 Abstract

For elucidating molecular structure and dynamics in solution, NMR experiments such as NOESY, ROESY and EXSY have been used excessively over the past decades, to provide interatomic distance restraints or rates for chemical exchange. The extraction of such information, however, is often prohibited by signal overlap in these spectra. To reduce this problem, *pure shift* methods for improving the spectral resolution have become popular. We report on *pure shift* EASY-ROESY experiments and their application to extract cross-relaxation rates, proton-proton distances and exchange rates. Homonuclear decoupling (*pure shift*) is applied in the indirect dimension using the PSYCHE or the *perfect*BASH technique, to enhance the spectral resolution of severely overcrowded spectral regions. The spectral quality is further improved by using a *gradient selected F*1-PSYCHE-EASY-ROESY, which produces significantly less t_1-noise than the experiment used previously, as also demonstrated by employing the recently introduced SAN (signal-artefact-noise) plots. Applications include

the quantification of distance restraints in a peptide organocatalyst and the extraction of a number of distance restraints in cyclosporine A, which were previously not available for analysis, because they were either located in overcrowded spectral regions or hidden under t_1-noise. Distances extracted and exchange rates obtained are accurate. Also, the 2D *gradient-selected F*1-*perfect*BASH-EASY-ROESY with the additional gradient selection proposed herein, which is superior in terms of sensitivity, can be used to accurately quantify cross-relaxation.

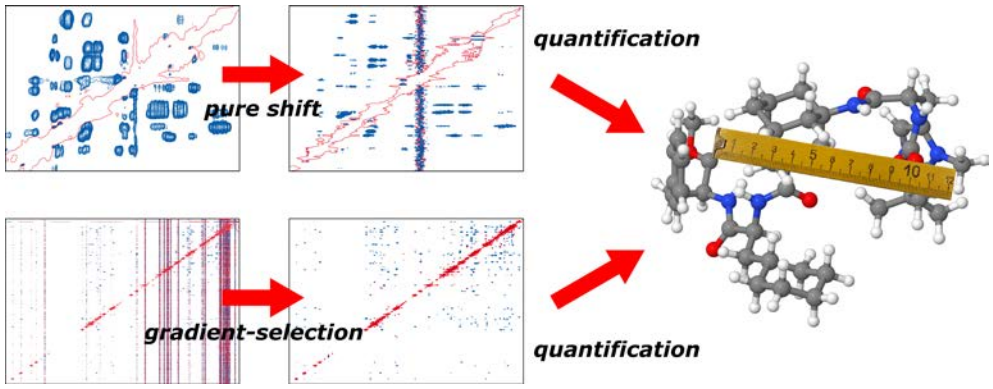

2 Highlights

- *pure shift* EASY-ROESY becomes quantitative!
- improvement of spectral resolution in EASY-ROESY spectra using *F*1-PSYCHE and *F*1-*perfect*BASH homonuclear decoupling
- quantification of cross-relaxation and chemical exchange in overcrowded spectral regions
- attenuated t_1-noise traces due to gradient selection
- applications to a peptidic organocatalyst and cyclosporine A

3 Introduction

The crucial key to understand physiological effects of active substances, catalytic reactions or functional materials is their three-dimensional structure. Hence the elucidation of molecular three-dimensional structure has become a pivotal element in chemical research. NMR spectroscopy is a popular and efficient tool for the structure elucidation in solution, since it provides rich information about the interatomic bonding network as well as on molecular geometry. The most commonly measured parameters which provide information about the spatial structure are *J*-couplings [1-4], the Nuclear Overhauser Effect (NOE) and Residual Dipolar Couplings (RDCs). In particular, correlations between nuclei that feature mutual longitudinal cross-relaxation via dipolar couplings (NOE) encode

for their internuclear distances [5-9]. Especially for medium-sized compounds, like the peptides investigated herein, the zero-crossing of the NOE can impede its use for this purpose. Thus resorting to transversal relaxation and employing rotating-frame Overhauser effect (ROE) measurements has proven beneficial for these cases[10-12]. Challenges arise due to the spin-lock involved leading to off-resonance effects and TOCSY (total correlation spectroscopy) transfer[13-20]. A remedy for these issues is the jump-symmetrized ROESY (JS-ROESY)[19]. For its implementation with adiabatic spinlocks called EASY-ROESY[21], it was shown previously that accurate distances and exchange rates can be obtained. This experiment shares a particularly useful property of ROESY spectra in general, namely that NOE/ROE can be differentiated from chemical exchange irrespective of the size of the compound investigated.

The cross-relaxation rates required for distance determination or the exchange rates for quantifying chemical exchange are easily extracted from the signal integrals observed in NOESY or ROESY spectra, if these signals are well separated from each other as well as from artefacts caused by the experimental technique. Even for moderately sized systems, however, signal overlap can easily interfere with signal integration. In addition, informative NOE/ROE peaks are usually comparably weak ($\sim r^{-6}$), rendering spectral artefacts a considerable problem during data analysis.

Signal overlap often becomes a problem if homonuclear *J*-couplings lead to broad overlapping multiplet patterns or direct *J*-correlation cross-peaks with unfavourable double anti-phase dispersive line shape. The latter are usually referred to as zero-quantum or COSY-artefacts. Since both effects originate from *J*-coupling evolution, these may be avoided, if the *J*-coupling evolution is suppressed in one or both spectral dimensions. This can be achieved with the incorporation of *pure shift* techniques[22-25] into NOESY and ROESY experiments, as an alternative to using Thrippleton-Keeler filtration[26, 27]. *Pure shift* approaches attempt to collapse homonuclear multiplets into singlets, thus reducing spectral overlap and further supressing signals with anti-phase homonuclear *J*-pattern. It was realized, that *pure shift* techniques therefore may support the more accurate extraction of structural constraints, including relaxation time constants[28, 29], heteronuclear and homonuclear *J*-couplings[30-39], RDCs[30, 31, 34, 39-42], chemical exchange kinetics[43] as well as NOEs[44, 45].

For quantification of the NOE from *pure shift* spectra, it was previously demonstrated, that band-selective techniques[44] or Zangger-Sterk[45] approaches can yield accurate distance data. Depending on the system to study, however, these techniques may not be the most powerful *pure shift* approaches available to date, for investigating small to intermediate sized molecules.

In this paper, we show for a series of *pure shift* ROESY experiments that accurate distance information can be obtained from the high-resolution spectra they provide. We use 2D-EASY-ROESY experiments with PSYCHE[46] and *perfect*BASH[47] homonuclear decoupling in *F*1 to extract cross-relaxation rates and subsequently to determine interproton distances from overcrowded 2D-EASY-ROESY spectra. The *F*1-PSYCHE-EASY-ROESY experiment was already used qualitatively during

the study of a peptide organocatalyst[48], to resolve the challenging aliphatic spectral region[49], whereas a quantification of distances was not attempted at that time. Here we show that the quantitative extraction of distance restraints in such challenging systems with overlapping spectra is possible, using the *F*1-PSYCHE-EASY-ROESY experiment. For the closely related *F*2-PSYCHE-EXSY experiment, it was recently shown[43], that it can be utilised to quantify exchange kinetics, yet it should be noted that chemical exchange, as compared to NOE in small molecules, produces a much more favourable cross-peak to diagonal peak intensity ratio for quantitative analysis, thus it would be risky to conclude from this data, that PSYCHE decoupled spectra are also suitable for the quantification of distance information from NOESY.

Furthermore we discuss a 2D *gradient-selected* (GS)[50, 51] *F*1-PSYCHE-EASY-ROESY pulse sequence, which attenuates unfavourable t_1-noise traces and allows for quantification of previously hidden or distorted NOE cross-peaks more accurately. Finally we use the *perfect*BASH homonuclear decoupling technique[47] to enhance the overall sensitivity and extract interproton distance restraints in the *gradient-selected F1-perfect*BASH-EASY-ROESY approach we further present.

4 Pulse sequence design

In the following chapter we discuss the aim, the experimental design and the working principle of the *pure shift* EASY-ROESY experiments used, starting with the already published *F*1-PSYCHE-EASY-ROESY experiment and continuing with the developments using gradient selection during the EASY-ROESY mixing step. Additionally, we present an EASY-ROESY experiment with *perfect*BASH homonuclear decoupling in *F*1 and gradient selection.

For a modest number of well separated proton signals the 1D versions of NOESY or ROESY with selective saturation or inversion of a narrow spectral region and observing the effects on the spins outside of this frequency region are the method of choice to probe cross-relaxation. These techniques will, however, be of limited use with increasing molecular complexity leading to many overlapping proton multiplets, while in 2D versions of NOESY or ROESY overlapped peaks may be dispersed in two frequency dimensions. The potential issues discussed above remain in place, though. Consequently, several NOESY and ROESY experiments utilizing a *pure shift* technique for homonuclear decoupling were published [40, 44, 45, 47, 49, 52-55].

In modern *pure shift* experiments the homonuclear *J*-coupling evolution is refocused with the aid of a spin subset selection, which discriminates between diluted active spins used for detection and the majority of passive spins, which are manipulated to achieve the decoupling effect. Techniques presented for discrimination are based either on frequency selection (BASH)[53, 56], isotope filtering with a nucleus with low natural abundance (BIRD)[57], simultaneous spatial and frequency selection (Zangger-Sterk)[58] or statistical methods (PSYCHE)[46]. The PSYCHE technique (*Pure Shift Yielded by Chirp Excitation*) provides encouraging results in terms of sensitivity, decoupling quality

and attenuation of signal contributions originating from strong coupling. These properties led to extensive applications in 1D and 2D experiments [29, 33, 36, 37, 42, 43, 49, 59-61]. Herein we apply the PSYCHE homonuclear decoupling in EASY-ROESY experiments for homonuclear decoupling of the indirect dimension *F*1.

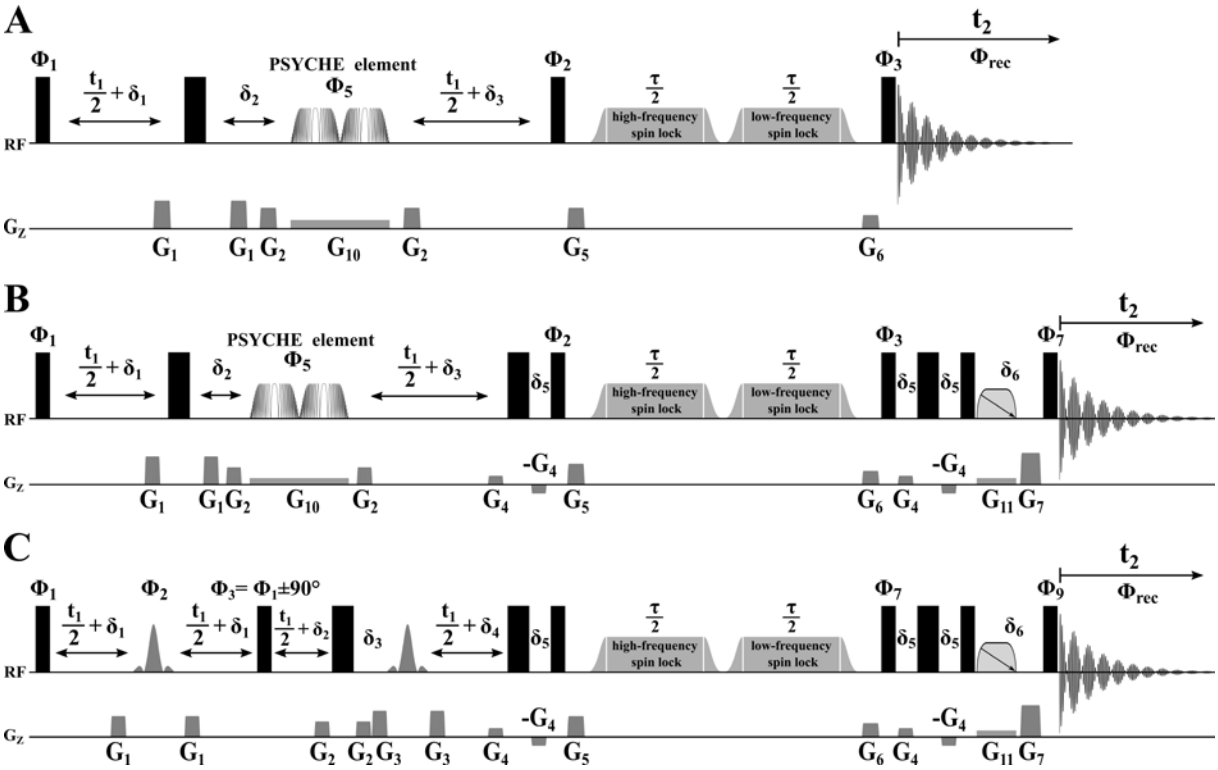

Figure 1: Pulse sequence schemes for (A) the *F1*-PSYCHE-EASY-ROESY experiment[49], (B) the *gradient-selected F1*-PSYCHE-EASY-ROESY experiment and (C) the *gradient-selected F1-perfect*BASH-EASY-ROESY experiment. Narrow and wide rectangles represent hard 90° and 180° pulses, respectively. The double trapezoid corresponds to low-power chirp pulses of small flip angle, which sweep frequency in opposite directions simultaneously (*PSYCHE* element). Broad rectangles in gray are low- and high-field spinlocks (SL) of *τ/2* duration, half-Gaussian shaped pulses are used as adiabatic ramps. Grey shapes in sequence (C) are selective pulses. Thrippleton-Keeler elements are indicated by a single trapezoid with diagonal arrow. The gradients G_1, G_2 and G_3 are used for coherence selection within the homonuclear decoupling element, G_4 is used for phase en- and decoding, the gradients G_5, G_6 and G_7 are purge gradients and G_{10} and G_{11} are weak gradients during the PSYCHE element and the Thrippleton-Keeler filter. In pulse sequence (A) the delays δ_1 through δ_3 are $\delta_1 = p_{17} + d_{16}$, $\delta_2 = 2p_{17} + 3d_{16}$ and $\delta_3 = p_{17} + 2d_{16}$, in (B) δ_1 to δ_5 are $\delta_1 = p_{17} + d_{16}$, $\delta_2 = 2p_{17} + 3d_{16}$, $\delta_3 = p_{17} + 2d_{16}$, $\delta_4 = p_{18} + d_{16}$ and $\delta_5 = p_{42} + p_{19} + 2d_{16}$ and in sequence (C) these are $\delta_1 = p_{17} + d_{16}$, $\delta_2 = 2p_{17} + 3d_{16}$, $\delta_3 = p_{17} + 2d_{16}$, $\delta_4 = p_{18} + d_{16}$, $\delta_5 = p_{42} + p_{19} + 2d_{16}$ and $\delta_6 = p_{42} + p_{19} + 2d_{16}$, where p_{17} to p_{19} are the durations of the gradient pulses, p_{42} the duration of the Thrippleton-Keeler element and d_{16} is a recovery delay. In all pulse sequences scalar coupling evolution during t_1 is refocused before the ROESY mixing step, while chemical shifts have evolved for t_1. Phase cycling: All pulse phases are x unless other denoted. (A) Φ_1 = x –x, Φ_2 = 8(x) 8(–x), Φ_3 = 4(x) 4(–x), Φ_5 = x x y y –x –x –y -y and Φ_{rec} = x –x –x x –x x x –x –x x x –x x –x –x x. (B) Φ_1 = x –x, Φ_2 = 16(x) 16(–x), Φ_3 = 8(x) 8(–x), Φ_5 = x x y y –x –x –y -y, Φ_7 = 4(x) 4(–x) and Φ_{rec} = x –x –x x –x x x –x –x x x –x x –x –x x –x x x –x x –x –x x x –x –x x –x x x –x. (C) Φ_1 = x –x, Φ_2 = x x y y, Φ_3 = y –y y –y, Φ_7 = 8(x) 8(–x), Φ_9 = 4(x) 4(–x) and Φ_{rec} =x –x –x x –x x x –x –x x x –x x –x –x x.

4.1 2D *F*1-PSYCHE-EASY-ROESY

The pulse sequence in Figure 1A shows the 2D *F*1-PSYCHE-EASY-ROESY experiment we have published previously[49]. The *J*-coupling evolution is refocused just before the beginning of the EASY-ROESY mixing element, whereby chemical shifts have evolved for t_1. This implementation results in 2D-EASY-ROESY spectra showing only chemical shifts in *F*1 and both chemical shifts and *J*-splittings in the direct dimension *F*2. The suppression of *J*-coupling effects in *F*1 is accompanied by an overall sensitivity loss which usually is in the range of 80 - 90%, depending on the applied flip angle of the PSYCHE.

While we chose to apply the PSYCHE homonuclear decoupling in the indirect dimension *F*1, alternative *pure shift* implementations with PSYCHE or other techniques in the direct dimension *F*2 are conceivable and have been exploited in recent literature [43-45, 49]. For *F*2 homonuclear decoupling either *real-time* decoupling during acquisition[56, 62, 63] or the interferogram-based acquisition scheme[58] are applied to construct a direct dimension with *pure shift* resolution. The latter scheme adds a further pseudo-dimension, acquiring the FID in short *data-chunks* and requires special post processing of the raw data. Furthermore, integrals have to be corrected to account for relaxation effects and chunking sidebands in order to obtain accurate cross-relaxation rates[45]. The less time consuming *real-time* decoupling utilised by McKenna and Parkinson[44] might accumulate effects from pulse imperfection during the multiple refocusing pulses and is thus not expected to lead to accurate cross relaxation rates. In contrast the implementation of *F*1 homonuclear decoupling promises the advantage of avoiding chunking artefacts. Thus we expect the *F*1-homonuclear decoupling to be the more favourable implementation for extraction of accurate cross-relaxation data, with the additional benefit, that it requires only standard processing methods. However, it should be noted, that homonuclear decoupling in the indirect dimension is only a reasonable choice, if an appropriate spectral resolution in *F*1 is achieved by choosing a rather large number of increments.

4.2 2D *gradient-selected F*1-PSYCHE-EASY-ROESY

When applying the EASY-ROESY experiment with PSYCHE homonuclear decoupling in *F*1, sharp line shapes in the indirect dimension and hence an enhanced resolution can be achieved. We have previously used this superior resolution to track down a catalyst-substrate interaction[49]. Already in that study we observed that the quality of spectra was reduced by the occurrence of intense noise traces along the indirect dimension *F*1, so called t_1-noise, at chemical shifts of intense protons signals. These stem from incomplete cancellation of magnetisation during phase cycling. Such imperfections arise from the combined effect of instrumental instabilities [64, 65] and experiment repetition delays which are a compromise between full spin system relaxation and short experiment duration. For 2D-NOESY and 2D-ROESY experiments, the biggest source of magnetisation to be suppressed via phase cycling is the build-up of magnetisation via T_1-relaxation during mixing, which has not been frequency

labelled during the initial evolution period t_1. Such t_1-noise is already a considerable problem in standard NOESY and ROESY. The challenge becomes even bigger for *pure shift* experiments which only observe between 1% and 20% of the initial magnetisation (depending on the method and exact parameters chosen), while being subject to the same intensity of t_1-noise as the experiment without homonuclear decoupling. In particular for strong proton signals, e. g. methyl groups, these intense noise traces overlap with the desired low-intensity NOE signals. This interferes with the precise extraction of distances and obscures weak or medium-sized NOE contacts, rendering them practically unobservable. A similar problem was previously encountered in 1D selective NOE measurements, in which subtraction artefacts interfered with the extraction of weak NOE contacts. Here gradient selection across the mixing time yields considerably cleaner spectra than the phase cycled experiments[66]. The signal-to-noise loss of a factor of two that resulted from such gradient selection was more than compensated for by the improved spectral quality. This was also implemented into semi-selective[50] and non-selective[51] homonuclear 2D experiments. With this in mind, we designed a new 2D *F*1-PSYCHE-EASY-ROESY pulse sequence with gradient selection across the EASY-ROESY mixing step by introducing gradient en- and decoding steps - both incorporated in a spin echo - before and after the mixing step. A number of different implementations were tested as detailed in chapter 5.10 of the SI, with the one shown in Figure 1B giving the best results in terms of t_1-noise attenuation, phase distortions and sensitivity loss. The combination of gradients with States-TPPI[67] quadrature encoding in *F*1 requires the addition of a *z*-filter after gradient decoding in order to obtain 2D spectra with double absorption line shape (see chapter 5.1 of the SI for further explanation). For this we chose a Thrippleton-Keeler element[26] to avoid phase-distortions in *F*2 by *J*-coupling evolution during the decoding echo. With the pulse sequence presented herein at least two scans per t_1-increment are required. Finally it should be noted that PSYCHE itself may introduce COSY-like responses in the EASY-ROESY spectra. These are observed at the average chemical shift of two coupled protons in *F*1. These artefacts are caused by an incomplete attenuation of COSY-like coherence transfer during the PSYCHE element applying the *spatio-temporal* averaging concept and thus occur in particular for coupled protons with small chemical shift differences (see chapter 5.9 in the SI for a detailed analysis).

4.3 2D *gradient-selected F*1-*perfect*BASH-EASY-ROESY

The main drawback of the enhanced spectral resolution and t_1-noise attenuation by the PSYCHE homonuclear decoupling and gradient selection is the reduced overall sensitivity. This may prevent the observation of NOE contacts by pushing them below noise-level in particular for long-range NOEs. Alternative *pure shift* techniques, such as the *multi-slice excited* Zangger-Sterk experiment (*nemo*-ZS)[38], band selective homonuclear decoupling (BASH)[56] or PEPSIE (*Perfect-Echo-Pure-Shift-Improved-Experiment*)[68] are able to compete with PSYCHE in terms of sensitivity, or even outperform it. Up to date, techniques based on band selective homonuclear decoupling provide the

highest sensitivity. BASH based homonuclear decoupling techniques use frequency selective soft pulses and make use of frequency differences between coupled protons to achieve the decoupling. Homonuclear decoupling is only achieved though, if only one single proton from a scalar coupling network (or several isolated protons belonging to different coupling networks) resonate/s within the frequency band of the selective pulse. If this condition can be fulfilled, BASH homonuclear decoupling works efficiently and causes no additional sensitivity loss. The BASH method was mostly used for α-peptides [40, 53, 55, 69-71], but applications to small DNA fragments [44, 72] or oligosaccharides [73] were also reported. In α-peptides the backbone α- and amide proton frequencies are usually well separated from each other and from the sidechain protons, hence either the α- or the amide protons can be selected and subsequently decoupled from other protons.

Recently it could be shown in two independent studies, that the combination of the Perfect-Echo experiment [74, 75] with band selective homonuclear decoupling loosens the requirements with respect to spectral signal clustering[47, 76]. Utilizing the Perfect-Echo-BASH or *perfect*BASH homonuclear decoupling element allows for the decoupling of two mutually coupled protons in one selectively irradiated spectral region. In the case of α-peptides *perfect*BASH enables simultaneous homonuclear decoupling of the α- and amide protons. The generalized *perfect*BASH principle can be used in 1D experiments, as well as for decoupling of the indirect dimension in a variety of homonuclear 2D experiments like TOCSY, NOESY, ROESY and several CLIP-COSY variants[47]. In a previous publication we proposed the *F*1-implementation of the *perfect*BASH homonuclear decoupling scheme into an EASY-ROESY experiment [47], however quantification of this experiment was not attempted nor discussed. The pulse sequence applied herein (Figure 1C) is an extended version of the previously published *F*1-*perfect*BASH-EASY-ROESY, which includes gradient selection over the EASY-ROESY mixing-step and the final z-filter. For experiments with *perfect*BASH decoupling one should be aware that the line widths in the decoupled dimension may be broader than those from experiments decoupled by other *pure shift* techniques acquired under the same conditions. This is due to the doubled evolution time within the homonuclear decoupling block. Furthermore it is noteworthy to mention, that the *perfect*BASH homonuclear decoupling will only work in the indirect dimension *F*1 of the EASY-ROESY experiment. For the hypothetical *F*2-*perfect*BASH-EASY-ROESY additional COSY cross-peaks are expected, provoked by the in-phase coherence mixing of the underlying perfect echo. This is a property exploited in the CLIP-COSY mixing scheme [77].

5 Results and discussion

In the following three sections we show the application of our three *pure shift* EASY-ROESY experiments with the aim to extract NOE-derived distances and exchange rates and discuss the necessary conditions for reliable quantification. It should be mentioned here, that the scope of this discussion is restricted to the extraction of cross-relaxation rates, interproton distances as well as exchange rates from challenging spectra. Potential improvement of structural models utilizing these new or more accurately determined interproton distance restraints is beyond the scope of this paper.

5.1 PSYCHE-EASY-ROESY: The tetrapeptide - *1R,2R*-cyclohexanediol system

To determine whether or not 2D *F*1-PSYCHE-EASY-ROESY experiments can be used for distance quantification in small to intermediate sized molecules, we first investigated the previously published version of the experiment (Figure 1A), using the tetrapeptide system already studied. In terms of spectral crowding, this system presents a notable challenge, since 46 protons of the peptide and the *R,R*-diol (highlighted in blue in Figure 2e) resonate in 33 individual signals within 1.4 ppm. As illustrated in Figure 2a, this results in significant peak overlap in the 2D EASY-ROESY spectrum. As described earlier, the spectral overlap can be significantly reduced using *F*1-PSYCHE decoupling, as shown in Figure 2b, reducing the overlap for many cross-peaks such as those highlighted in green and orange. Thus we acquired a mixing-time series of 2D *F*1-PSYCHE-EASY-ROESY experiments with sufficiently long recovery delay d_1 to assure full relaxation for the analyte ^{1}H signals. For quantification we used the method of integrating the 2D-EASY-ROESY spectra within several extracted 1D spectra, which we obtained by extracting *F*2-traces at the peak maximum in the indirect dimension *F*1[78]. This approach assumes uniform linewidths in *F*1, which is realized here to a good extent, by suppressing *J*-multiplicity and by using experimental conditions under which the linewidth in *F*1 is determined by the digital resolution and by the apodization applied, and not by the natural linewidths. For data analysis the integrated cross-peak intensities of each mixing-time step were normalised with the corresponding diagonal-peak integral only in the same *F*2-trace according to $a_1(\tau_m)$ described in the paper of Macura[79].

In general, the internal normalization enables the extension of an initial rate analysis of the data to much longer mixing-times. In 1D NOESY/ROESY experiments this analysis is referred to as PANIC approach[80], a terminology we use in the following discussions. With the normalization of the cross-peak integrals with the corresponding diagonal integral in the same row (same chemical shift in *F*1) we further achieve the elimination of the proton specific T_2-relaxation weighting in t_1 and further proton specific T_2 and offset weighting effects introduced by the PSYCHE homonuclear decoupling element itself (see SI for a discussion of the β-factor, chapter 2.1 and 5.8). Quantification of the mixing-time series gave a linear behaviour between the normalised NOE cross-peak integrals

(Overhauser enhancement) and the mixing time τ_m in the PANIC plots, as illustrated in the two representative plots in Figure 2c and d. These two plots were constructed by quantification of the two NOE cross-peaks highlighted in Figure 2b) and belong to a diastereotopic proton pair (orange, d) and a vicinal proton pair with equatorial-axial relationship (green, c) in the cyclohexyl-group, respectively.

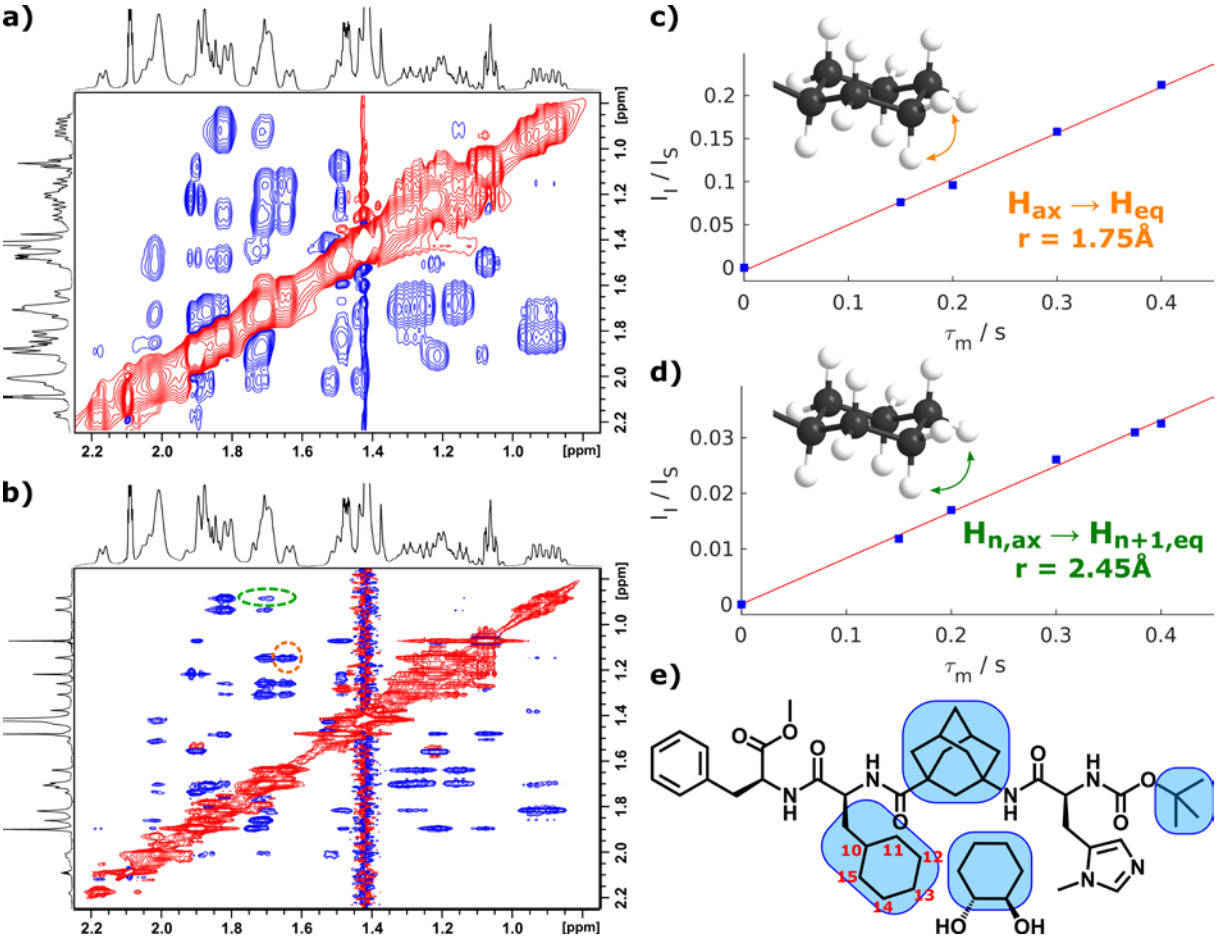

Figure 2: Aliphatic region of the tetrapeptide - *1R,2R*-cyclohexane-diol system in toluene-d_8 (structure shown in (e) with proton assignment of the cyclohexyl moiety) acquired with (a) the 2D-EASY-ROESY experiment and (b) with the 2D *F*1-PSYCHE-EASY-ROESY experiment. Both spectra were measured at 700.17 MHz under non-quantitative conditions (recovery delay d1=1.5 s) and a mixing-time of 300 ms. The EASY-ROESY spectrum without *pure shift* in *F*1 in (a) was acquired with less spectral resolution in *F*1 than the spectrum with *pure shift* in (b), however increasing the resolution in *F*1 will not change the situation of overlapped NOE cross-peaks. For the cross peaks marked in green and orange the PANIC plots are shown in (c) and (d). These can only be resolved with the aid of PSYCHE homonuclear decoupling in *F*1.

For the tetrapeptide - *R,R*-diol system, clear indications for conformational flexibility and molecular aggregation exist. Since the principle goal of this chapter is not to reinvestigate the structure of the tetrapeptide itself nor the interactions between tetrapeptide and diol, but rather to study whether the 2D *F*1-PSYCHE-EASY-ROESY is suitable for quantitative proton-proton distance determination, we restrict the data discussed in this chapter to distances for which we expect little influence by flexibility and for which we expect a good reference to be available by computational methods. In the 2D *F*1-PSYCHE-EASY-ROESY spectra a lot of NOE contacts from the cyclohexyl moiety are resolved,

which belong to rigid and known interproton distances. Through the enhanced spectral resolution of the 2D *F*1-PSYCHE-EASY-ROESY, integration of these cross-peaks can be easily performed including diastereotopic protons usable for internal calibration, which were not accessible previously when we relied on 1D-NOE experiments without homonuclear decoupling[49]. From the 2D *F*1-PSYCHE-EASY-ROESY mixing-time series we could quantify six NOE cross-peaks belonging to diastereotopic proton pairs and found distances in the expected range of 1.73 - 1.84 Å. Further we analysed cross-peaks of vicinal proton pairs, which have an equatorial-axial relationship ($H_{n,ax} \rightarrow H_{n+1,eq}$, r = 2.45 Å) as well as cross-peaks of two axial protons four chemical bond apart (1,3-diaxial relationship, $H_{n,ax} \rightarrow H_{n+2,ax}$, r = 2.67 Å). In both cases we could extract interproton distances from the mixing-time series of the 2D *F*1-PSYCHE-EASY-ROESY experiment close to the expected values, which are within the systematic errors of interproton distances determined from cross-relaxation experiments[81-84]. The expected values of the interproton distances were extracted from an MMFF94[85] energy minimized monosubstituted cyclohexane.

Table 1: Proton-proton distances within the cyclohexyl moiety (proton assignment in Figure 2e) of the tetrapeptide determined with a mixing-time series of the 2D *F*1-PSYCHE-EASY-ROESY experiment.

H_A	H_B	$r_{exp,A\rightarrow B}$ / Å	$r_{exp,B\rightarrow A}$ / Å	r_{model} / Å[a]
H11ax	H11eq	1.76(1)		
H12ax	H12eq	1.84(1)		
H13eq	H13ax	1.75(1)[b]	1.73(1)	1.75
H14ax	H14eq	1.81(1)		
H15ax	H15eq	1.75(1)		
H11ax	H12eq	2.33(3)		
H12ax	H11eq	2.60(2)		
H12ax	H13eq	2.42(3)		
H13ax	H12eq	2.28(3)		
H13ax	H14eq	2.28(3)		2.45
H14ax	H13eq	2.26(4)		
H14ax	H15eq	2.60(2)		
H15ax	H14eq	2.37(1)		
H11ax	H13ax	2.55(2)	2.62(5)	
H13ax	H15ax	2.62(5)	2.62(2)	2.67

[a] Determined with an energy minimized (MMFF94)[85] monosubstituted cyclohexane structure model.

[b] Used as reference distance

Based on these promising results we extracted all distances from NOE contacts, which were sufficiently resolved. In sum we could extract 74 distance restraints from the mixing-time series of the 2D *F*1-PSYCHE-EASY-ROESY experiment, which, on one hand, is an increase of the number of accessible contacts by a factor of four, as compared to our previous investigation[49]. On the other hand, we now have access to distance restraints not exclusively from the peptide backbone, but rather from different parts of the peptide. The distances extracted outside the cyclohexyl moiety must, however, be interpreted with caution due to potential structural changes caused by aggregation and degradation processes. Thus a further investigation and structural study is outside of the scope of this work.

5.2 2D *gradient-selected F*1-PSYCHE-EASY-ROESY

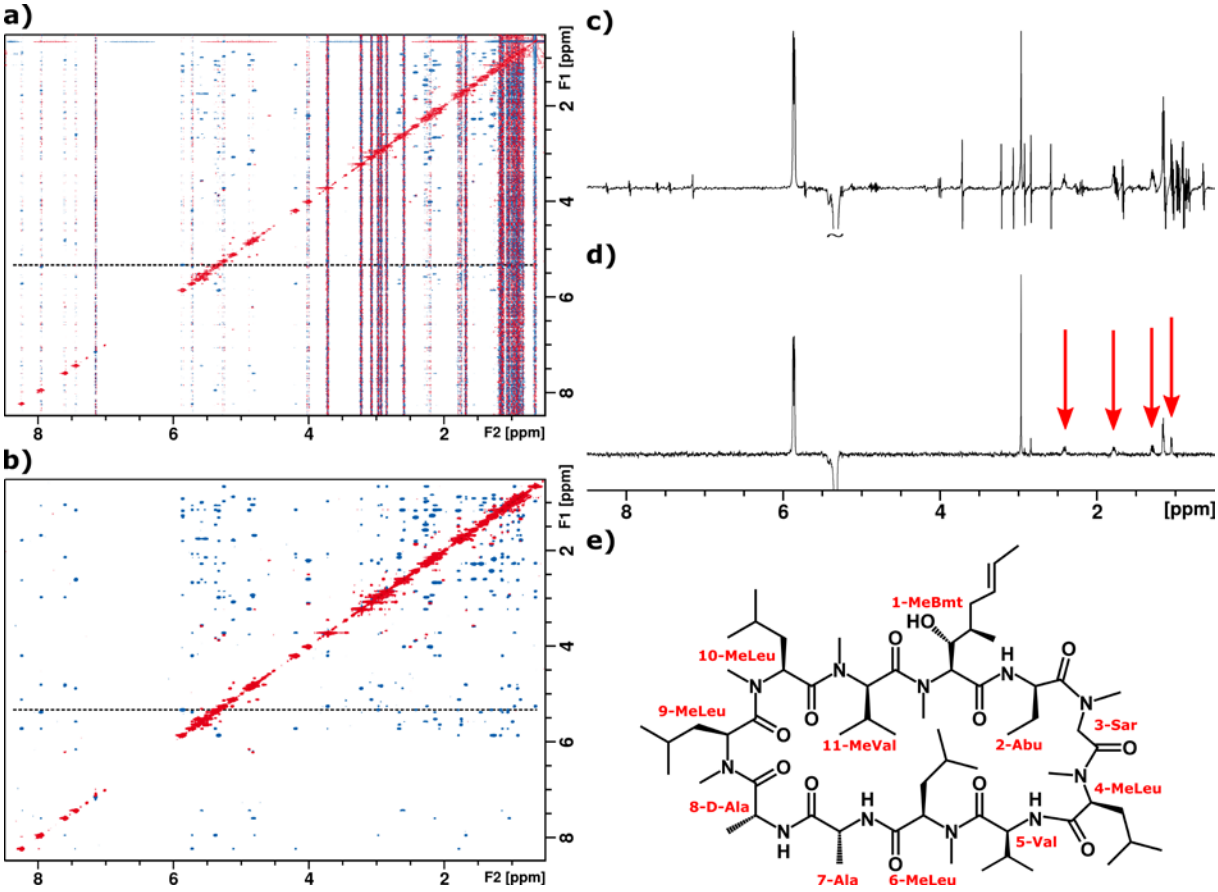

Figure 3: 2D-EASY-ROESY spectra of cyclosporine A in benzene-d_6 (structure shown in (e)) acquired with (a) the 2D *F*1-PSYCHE-EASY-ROESY experiment and (b) with the 2D *gradient-selected F*1-PSYCHE-EASY-ROESY experiment. Both spectra were measured at 600.3 MHz under non-quantitative conditions (recovery delay d1 = 2 s) and a mixing-time of 300 ms, all other acquisition parameters are the same as for the quantitative experiments (see SI, chapter 1.4). In c) and d) the *F*2-traces extracted from both spectra in a) and b) at the peak maximum of proton 10-α in *F*1 (black dashed lines) are shown. The marked weak to medium sized NOE responses are clearly visible in d), which cannot be seen in c).

In the previous chapter we analysed, whether we can extract cross-relaxation rates and interproton distances from a mixing-time series of a 2D-EASY-ROESY experiment with PSYCHE homonuclear

decoupling in the indirect dimension, with the aim to get access to structural constraints even if the spectral region is severely overcrowded. As a test system, the tetrapeptide is quite challenging though, because of conformational averaging of all structural constraints as well as sample aggregation and degradation processes. Thus we decided to switch to the less complicated undecapeptide cyclosporine A (structure shown in Figure 3e) for further discussion. If 2D *F*1-PSYCHE-EASY-ROESY spectra are collected for this system according to the scheme in Figure 1a, a ROESY spectrum dominated by intense noise traces along the indirect dimension is obtained (Figure 3a). The occurrence of such noise traces, so-called t_1-noise, is a well-known phenomenon in 2D experiments in particular for intense proton signals, e. g. methyl groups. To remove these, we designed the new 2D *gradient-selected F*1-PSYCHE-EASY-ROESY experiment (pulse sequence B in Figure 1, for the pulse sequence design concept see the previous section). If we use this new pulse sequence to collect spectra for cyclosporine A with the same number of scans per t_1-increment, the intense noise traces, present in spectra acquired according to pulse sequence scheme A, are gone as shown in Figure 3b. To further illustrate the effect, representative *F*2-traces of the two spectra are shown in Figure 3c and d. Many of the NOE contacts, which were previously hidden under intense noise traces, are clearly visible now. To visualize and compare the improvement in quality of the 2D *gradient selected F*1-PSYCHE-EASY-ROESY (variant B) over the previous experiment (variant A) in a graphical manner, the very recently introduced *signal-artifact-noise (SAN)* plots [86] are applied. Herein the spectra are analysed with a distribution of point intensities, which are then sorted by their decreasing absolute values to construct a graphical representation of the signal, noise and artefact content. The constructed SAN-Plots of both *F*1-PSYCHE-EASY-ROESY spectra of cyclosporine A in Figure 3 (with and without *gradient selection*) are shown in Figure 4a and b. The comparison of the SAN plots nicely reflects the disappearance of the artefact region and thus clearly demonstrates the superior performance of the new experiment.

When we acquire the spectra under quantitative conditions with a recovery delay d_1 of at least five times the longest T_1 relaxation time constant, the attenuation of t_1-noise is less evident than in experiments with short relaxation delay, yet the suppression of t_1-noise still is significantly better than a quantitative 2D *F*1-PSYCHE-EASY-ROESY experiment, as expected. Since we showed in the previous section, that the 2D *F*1-PSYCHE-EASY-ROESY experiment according to Figure 1A is suitable for NOE quantification purposes, we were asking ourselves, if we can use the new 2D *gradient-selected F*1-PSYCHE-EASY-ROESY (variant B) as well to extract NOE distance restraints in a quantitative fashion. In contrast to the 2D *F*1-PSYCHE-EASY-ROESY pulse sequence (variant A), the coherence selection with gradients introduces further effects with (potential) impact on the absolute intensity of the proton peaks. Firstly, the maximum sensitivity which can be recovered with gradient selection is one half. Secondly, the pulse sequence in Figure 1B has similarities to experiments for the measurement of molecular diffusion. Thus diffusion and convection effects will additionally attenuate the peak intensities in these experiments. Diffusion and potential convection evolve during the mixing-time τ_m and thus influence the NOE build-up. During NOE analysis this

would lead to systematic errors in the cross-relaxation rates if no correction was applied. Since diffusion and convection affect the molecule as a whole, however, their influence on intramolecular cross-relaxation rates can be eliminated through internal normalization of the NOE cross-peaks with the corresponding diagonal-peaks, as already used during the NOE analysis of the pulse sequence variant A (2D *F*1-PSYCHE-EASY-ROESY, for theoretical analysis: see SI, chapter 5.1). It should be noted, that for weak intermolecular complexes, such as proposed for the tetrapeptide – *R,R*-diol system, this will not apply, since the different binding partners will feature different diffusional properties.

When applying the previously described approach of integrating extracted *F*2-traces for quantification, we obtained PANIC plots, which showed consistently good linearity ($r^2 \geq 0.95$). Using this procedure, we were able to extract a total of 226 proton-proton distances in a range up to 5 Å. Hereby we only utilised NOE responses which were sufficiently above the background noise level. For the purpose of evaluating if the experiment presented is suitable for quantitative NOE distance measurements, we decided to first investigate selected distance restraints of well-known geometries, which were found in the previous structural analysis of cyclosporine A dissolved in chloroform[87, 88]. Because we used a different solvent (C_6D_6) than the one used previously ($CDCl_3$)[88] we focused on moieties with little expected change in our comparison. The distances extracted from the 2D *gradient-selected F*1-PSYCHE-EASY-ROESY are in a good agreement with values expected for these geometries (SI, chapter 3.7). Indeed, although this brief comparison suggests that the distances determined with the 2D *gradient-selected F*1-PSYCHE-EASY-ROESY experiment are accurate, we subjected this central issue to a closer inspection. Thus, we also extracted interproton distances of the cyclosporine A sample applying two other approaches. We chose two selective 1D-ROESY variants, one with a *continuous-wave* spin-lock (CW-ROESY) and the other with the EASY-ROESY mixing. Both experiments select a narrow proton frequency band using a *pulsed field gradient selected selective spin-echo* and apply gradient selection (GS) over the ROESY mixing to improve spectral quality. Since these two ROESY experiments are based on selective refocusing, they only provide cross-relaxation data for protons, which are not overlapping with others. We acquired both kinds of 1D-ROESY spectra under variation of the mixing-time for the amide- and most of the α-protons as well as for all N-methyl groups and some protons of the sidechains (SI, chapter 1.6).

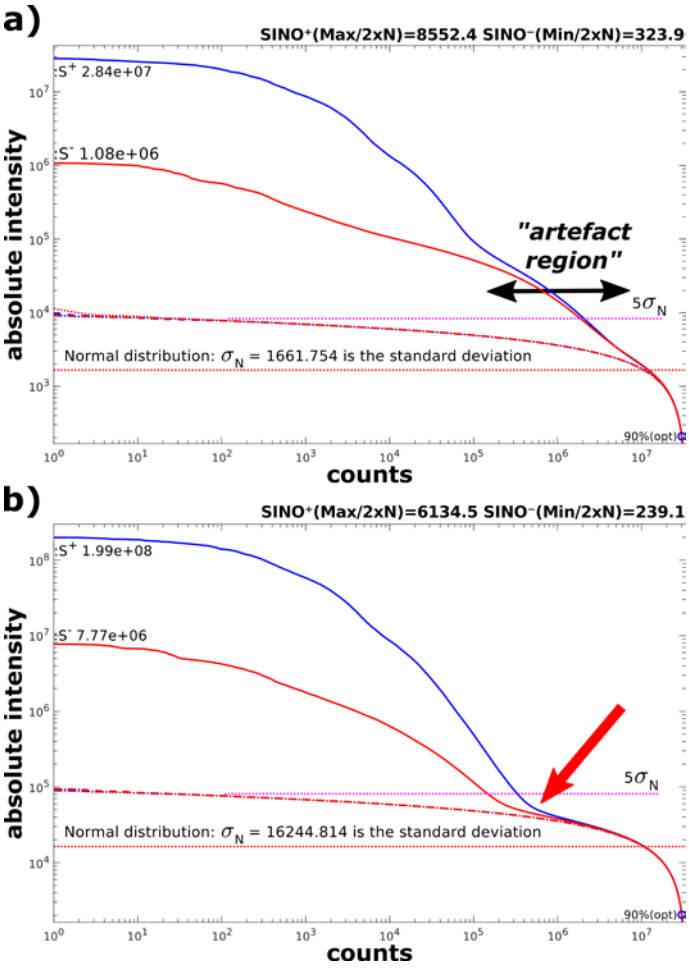

Figure 4: SAN-plots (signal/artifact/noise) constructed (a) from the 2D *F*1-PSYCHE-EASYROESY (variant A) and (b) from the 2D *gradient-selected F*1-PSYCHE-EASY-ROESY of cyclosporine A in C_6D_6. The corresponding spectra are shown in Figure 3. The SAN-plot (a) shows a quite smooth course of the positive *S*+ (solid blue) and the negative *S*- spectral points (solid red). This gradual transition between the signal and noise area (dashed-dotted red/blue) is caused by the intense t_1-noise present in the 2D *F*1-PSYCHE-EASY-ROESY spectrum (variant A), whose data points are located in the artefact region in between signals and background noise. In contrast to this is the SAN-plot (b). Here we can see a sharp edge between the signal and the noise region (marked with the red arrow) due to the efficient attenuation of t_1-noise and artefacts by gradient-selection. The comparison illustrates in a graphical representation the superior performance of the 2D *gradient-selected F*1-PSYCHE-EASY-ROESY experiment. The spectra were not acquired with the same receiver gain value, but with values optimized for the individual experiments. For a direct comparison of normalised peak intensities, see SI, chapter 5.3.

With the 1D *gradient-selected* CW-ROESY we had access to 126 interproton distances, out of which 108 were also available from the PSYCHE decoupled EASY-ROESY experiments. Applying the 1D *gradient-selected* EASY-ROESY we were able to extract 163 interproton distances, when selectively irradiating the same protons. From these experiments we can compare 126 interproton distances with the ones extracted from the 2D g*radient-selected F*1-PSYCHE-EASY-ROESY. The scatter plots (Figure 5) of both comparisons show nearly perfect matching of the interproton distances extracted with the different methods (RMSD values of 0.155 Å and 0.087 Å). The consistency between the data measured with 1D *gradient-selected* EASY-ROESY and the 2D *gradient-selected F*1-PSYCHE-

EASY-ROESY turned out to be even better than the comparison between the 1D *gradient-selected* CW-ROESY and the 2D *gradient-selected F*1-PSYCHE-EASY-ROESY (see Figure 5a and b). This fact, however, is not surprising as the same ROESY mixing element for cross-relaxation was applied. The CW-ROESY has indeed the best properties in terms of simultaneous suppression of longitudinal cross-relaxation and TOCSY transfer[19], but suffers from off-resonance effects. Nevertheless the attenuation of simultaneous TOCSY transfer and the averaging of offset effects is improved in the EASY-ROESY mixing scheme. However, the comparison between the 2D *F*1-PSYCHE-EASY-ROESY with both 1D ROESY variants indicates, that the accuracy of the extracted distances is less influenced by the PSYCHE homonuclear decoupling than by the type of ROESY mixing applied. With this we can conclude, that no further essential error sources beyond the existing approximations made to analyse cross-relaxation in general, namely the *isolated dipolar coupled proton pairs approximation*, the integration accuracy and the evaluation process are introduced by PSYCHE homonuclear decoupling. The acquisition of the 2D *gradient-selected F*1-PSYCHE-EASY-ROESY under quantitative conditions is accompanied with long measurement times up to 43 h per mixing-time, whereas the whole 1D *gradient-selected* EASY-ROESY data set could be measured in 29 h. However, the 1D version only gives access to distance restraints from protons, which could be sufficiently irradiated by selective refocusing pulses.

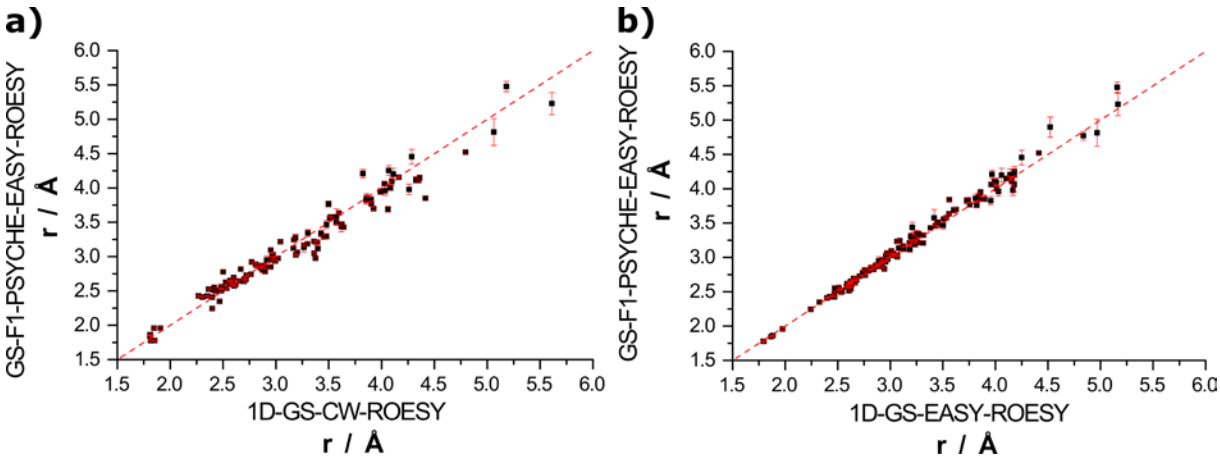

Figure 5: a) Comparison between proton-proton distances determined with the 2D *gradient-selected F*1-PSYCHE-EASY-ROESY and with the 1D *gradient-selected* CW-ROESY experiment (r^2 = 0.975, RMSD = 0.155 Å), b) comparison between proton-proton distances determined with the 2D *gradient-selected F*1-PSYCHE-EASY-ROESY and with the 1D *gradient-selected* EASY-ROESY experiment (r^2 =0.993, RMSD = 0.087 Å).

5.2.1 Extraction of chemical exchange rates

In NOESY or ROESY experiments, mixing of spin polarization may occur via cross-relaxation of dipolar coupled nuclei or via chemical exchange. When using ROESY experiments we can take advantage of the favourable property, that cross-peaks originating from chemical exchange can always be easily distinguished from those originating from cross-relaxation by their sign relative to the

diagonal peaks irrespective of the motional regime. Provided that TOCSY polarization transfer during the ROESY spin-lock can be suppressed sufficiently, cross-peaks with the same sign as the diagonal-peaks indicate slow chemical exchange between two species. For several slowly interconverting species, each one giving rise to an additional proton signal set, the risk of potential signal overlap increases, rendering the quantification of exchange increasingly challenging.

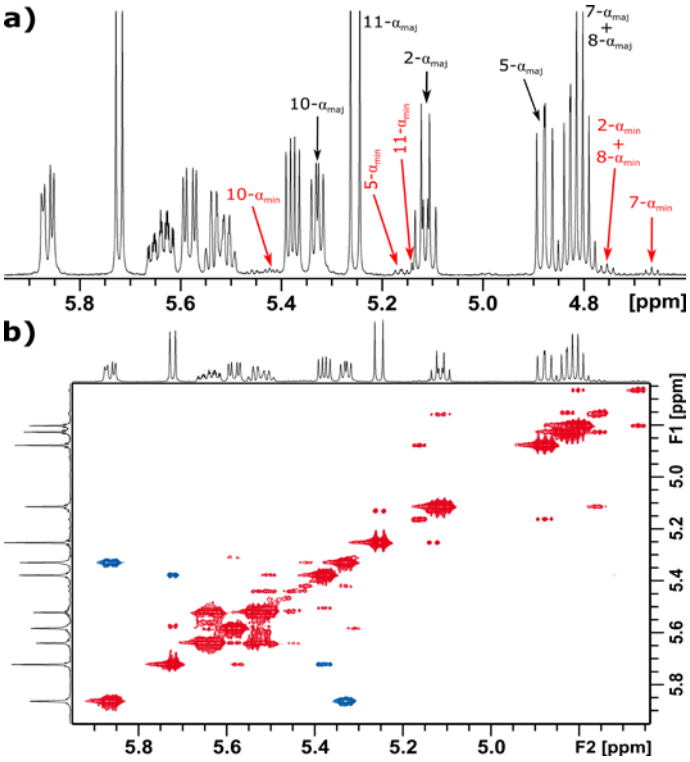

Figure 6: (a) H_α-proton region of cyclosporine A in benzene-d_6 (600.3 MHz) and (b) the same region in the 2D *gradient-selected F*1-PSYCHE-EASY-ROESY spectrum (600.3 MHz) at 300 ms mixing-time. In a) the red arrows highlight the *α*-proton signals of the minor conformer of cyclosporine A, the corresponding signals of the major conformer are marked in black. In b) the exchange peaks between the two conformers can be seen, which have the same sign as the diagonal peaks (visible NOE cross-peaks have an inverse sign).

The 2D *F*1-homodecoupled EASY-ROESY experiments discussed herein were found to be quite useful to resolve the proton signals of these different species. For cyclosporine A, a second minor conformer is described, which is in slow dynamic exchange with the major conformer at 300 K [87, 89-91]. In the 1D ^{1}H-spectrum of cyclosporine A, the existence of a minor conformer can be observed as a second proton signal set (Figure 6a) with smaller intensity (4-5 %). In addition, cross-peaks with the same sign as the diagonal-peaks could be observed in all ROESY experiments acquired (Figure 6b). So far we analysed the quantification of cross-relaxation data from 2D *F*1-PSYCHE-EASY-ROESY experiments and we could show the extraction of proton-proton distances with good accuracy. Thus we subsequently explored the quantification of chemical exchange of the two cyclosporine A conformers. The applicability for the extraction of exchange rates from a mixing-time series of a *F*2-PSYCHE-EXSY experiment could recently be proven using the full exchange matrix analysis[43]. We use the PANIC approach for straightforward elimination of the mixing-time dependent diffusion factor

(SI, chapter 4.1). The exchange rates extracted for *α*-protons and *N*-methyl-groups have similar values and are identical to the exchange rates determined with the 1D EASY-ROESY experiment (SI, chapter 4.2). For a few protons of the minor conformer the diagonal-peaks are sufficiently resolved in the 2D *gradient-selected F*1-PSYCHE-EASY-ROESY spectra such that the exchange rates of the reversed process can also be determined with the quantification procedure described before. Knowing the reversed exchange rate, the populations of the two conformers can be calculated. These are in excellent agreement with the ones which can be obtained by integration of the respective signals (which is not always possible).

Table 2: Exchange rates k_{AB}/ k_{BA} and the minor conformer population x_B of cyclosporine A in benzene-d_6 determined with the mixing-time series of the 2D *gradient-selected F*1-PSYCHE-EASY-ROESY experiment and the 1D *gradient-selected* EASY-ROESY experiment. Further extracted exchange rates and conformer population values can be found in the SI.

H	2D *Gradient-selected F*1-PSYCHE-EASY-ROESY			1D-EASY-ROESY
	k_{AB} / s^{-1}	k_{BA} / s^{-1}	x_B[a]	k_{AB} / s^{-1}
1-*α*	0.031(2)	--	--	0.033(2)
2-*α*	0.033(2)	--	--	0.033(1)
5-*α*	0.031(1)	1.04(7)	0.029(2)	--
7-*α*	0.032(3)	1.08(5)	0.029(3)	--
10-*α*	0.028(2)	1.08(8)	0.026(2)	0.029(3)
1-NMe	0.035(1)	1.06(4)	0.032(2)	0.038(1)
3-NMe	0.033(1)	1.14(3)	0.029(1)	0.036(1)
6-NMe	0.033(2)	--	--	0.037(1)

[a] Integration of sufficiently resolved signals of both the major and the minor conformer (5-*α:* 4.878/5.163 ppm, 3-NMe: 3.066/2.710 ppm) yields x_B = 0.04 - 0.05.

5.3 Enhancing the sensitivity: 2D *gradient-selected F*1-*perfect*BASH-EASY-ROESY

So far, we have discussed the resolution and spectral quality enhancements which can be achieved when applying PSYCHE homonuclear decoupling and gradient selection in EASY-ROESY experiments, with the aim to increase the number of distance restraints which can be extracted from challenging spectral regions. The main drawback of all these techniques is the loss in sensitivity, mainly by the *pure shift* element but also by gradient selection. This may prevent the observation of cross-relaxation within samples with a low amount of substance. In particular long-range NOE cross-peaks may be hidden by pushing them below noise-level. Interproton distances of long-range NOE contacts are usually error prone, caused by their inherent weak intensity and by the impact from spin-diffusion effects which often is non-negligible for these contacts[92]. In addition, there is a higher

propensity that these distances are biased by internal flexibility or relayed magnetisation transfer. Still, long-range contacts can contain valuable structural information, as they allow relating different structural elements. Even for shorter-range contacts the accuracy of cross-relaxation data extraction generally is improved with enhanced cross-peak intensity. For systems amenable to *perfect*BASH decoupling[47] (e.g. α-peptides), the EASY-ROESY experiment with the *perfect*BASH scheme for homonuclear decoupling in *F*1 (pulse sequence C in Figure 1) provides spectra with higher sensitivity than the 2D *F*1-PSYCHE-EASY-ROESY. Whether or not it is possible to extract quantitative information from the signal integrals of these Perfect-Echo[74] modified *pure shift* experiments was not evaluated so far, though.

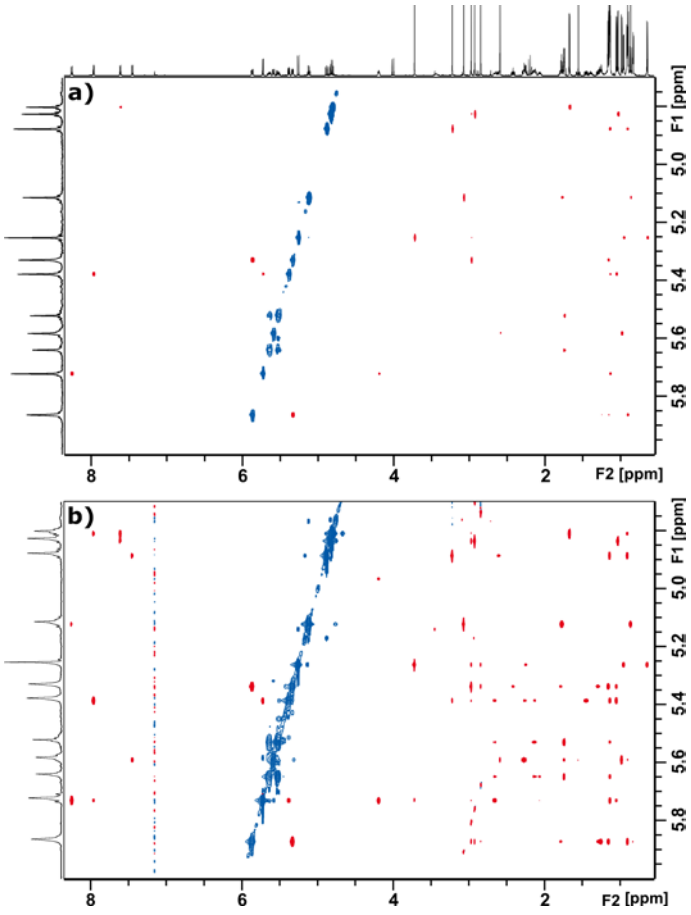

Figure 7: Comparison between two 2D *gradient-selected pure shift* EASY-ROESY spectra with homonuclear decoupling in *F*1 either using a) PSYCHE or b) *perfect*BASH. Both spectra were acquired at 600.3 MHz and with a mixing-time τ_m of 200 ms. In both spectra the same intensity level was used. Although *perfect*BASH enables the simultaneous decoupling of the amide- and the α–proton region, only the spectral region of the α–protons is shown in the indirect dimension *F*1.

Hence, for proof of principle, we also exemplarily analysed 2D *F*1-*perfect*BASH-EASY-ROESY spectra, to investigate the possibility of extracting distance restraints. The special band-selective character of *perfect*BASH enables simultaneous homonuclear decoupling of the amide- and α-proton region of α-peptides, such as cyclosporin A. In the case of the peptide catalyst *R*,*R*-diol system, the α-proton region is quite well resolved and thus not challenging while the amide-proton region is

overlapped by aromatic protons, which could not be decoupled with *perfect*BASH. Thus, we again chose the cyclosporine A sample for our study of integral quantification. Already when applying short mixing-times a clear advantage of *perfect*BASH decoupling becomes apparent: The signal-to-noise ratio of the NOE cross-peaks in the 2D *gradient-selected F*1-*perfect*BASH-EASY-ROESY spectra is notably better than in the PSYCHE decoupled experiments, allowing us to restrict the mixing-time series used to 250 ms as longest mixing time. The *perfect*BASH decoupled EASY-ROESY spectrum (Figure 7b) acquired with a mixing-time of 200 ms shows more NOE cross-peaks, which are sufficiently different from the background noise level, in comparison to a PSYCHE decoupled experiment (Figure 7a) with the same mixing-time and same intensity level for spectral representation. Furthermore, we were even able to observe NOE contacts for the minor conformer of cyclosporine A (SI, chapter 4.3).

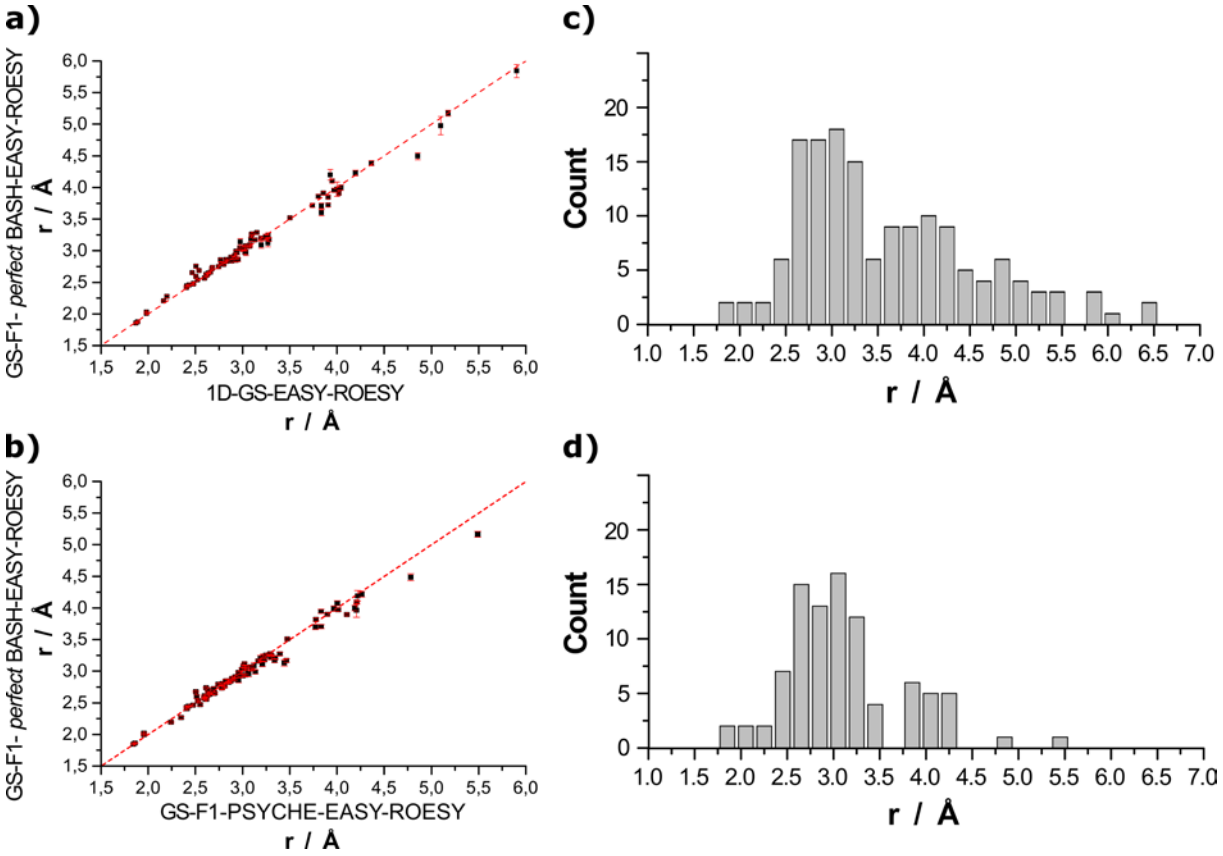

Figure 8: (a) Comparison of proton-proton distances determined with the 2D *gradient-selected F*1-*perfect*BASH-EASY-ROESY and the 1D *gradient-selected* EASY-ROESY experiment (R^2 = 0.994, RMSD = 0.089 Å) and (b) (a) comparison of proton-proton distances determined with the 2D *gradient-selected F*1-*perfect*BASH-EASY-ROESY and the 2D *gradient-selected F*1-PSYCHE-EASY-ROESY experiment (R^2 = 0.991, RMSD = 0.097 Å). Distribution of the interproton distance values extracted from the 2D *gradient-selected* EASY-ROESY spectra with homonuclear decoupling in *F*1 using (c) *perfect*BASH and (d) PSYCHE. The histogram in (d) contains only the distances from protons of the amide- and *α*-region, which could also be extracted with the 2D *gradient-selected F*1-*perfect*BASH-EASY-ROESY.

From the mixing-time series acquired, we could extract 153 interproton distances using the same procedure for quantification as previously described. As we have band selectively decoupled the amide- and the α-proton regions, the extracted distances are exclusively from these protons. Additionally, the three side-chain protons H_β, H_ε and H_η of the amino-acid 1-MeBmt as well as the two N-methyl protons of 1-MeBmt and 6-MeLeu fall into the selected region. With the mixing-time series of the 2D *gradient-selected F*1-*perfect*BASH-EASY-ROESY experiment we could find similar proton-proton distances restraints for the characteristic geometries in cyclosporine A as found using PSYCHE. Hereby we benefited from the enhanced sensitivity and hence the improved accuracy to determine distances bigger than 3 Å. Furthermore, the extracted distances from the 2D *gradient-selected F*1-*perfect*BASH-EASY-ROESY spectra are in good agreement with the distances determined with the *selective* 1D-ROESY experiments (Figure 8a) as well as with the 2D *gradient-selected F*1-PSYCHE-EASY-ROESY experiment (Figure 8b). In comparison to the PSYCHE decoupled EASY-ROESY experiment, the enhanced sensitivity of *perfect*BASH decoupling gave access to significantly more interproton distances from the selected amide- and *α*-proton region (153 versus 91). While long-range NOE contacts are generally more error prone due to their low intensity and should thus be interpreted carefully during structure calculation processes it is of note here, that the number of interproton distances above 3.5 Å (Figure 8c and d) is significantly increased.

6 Conclusion

In this paper we present the application of EASY-ROESY experiments with PSYCHE and *perfect*BASH homonuclear decoupling in the indirect dimension for the extraction of cross-relaxation rates, proton-proton distances and exchange rates. The enhanced spectral resolution obtained by PSYCHE homonuclear decoupling allows on the one hand a clearer qualitative distinction between different NOE contacts and on the other hand the extraction of cross-relaxation data even if severe spectral crowding is present. With the 2D *gradient-selected F*1-PSYCHE-EASY-ROESY pulse sequence presented, we could improve the quality of the 2D *F*1-PSYCHE-EASY-ROESY spectra by attenuation of t_1-noise. This was achieved by relying on gradient selection instead of phase-cycling for t_1-noise suppression, which facilitates the observation of weak to medium size NOE cross-peaks significantly. As an alternative to 2D *F*1-PSYCHE-EASY-ROESY, we improved an EASY-ROESY experiment with *perfect*BASH homonuclear decoupling in the indirect dimension which provides significantly higher sensitivity. This experiment allows the simultaneous homonuclear decoupling of two mutually coupled protons in one region (e.g. the amide- and *α*-proton region in peptides).

The presented 2D *F*1-PSYCHE-EASY-ROESY experiment was used to obtain proton-proton distances restraints for a peptide catalyst from a severely overcrowded aliphatic region, which previously was inaccessible for such kinds of analyses. The 2D *gradient-selected F*1-PSYCHE-EASY-ROESY and the 2D *gradient-selected F*1-*perfect*BASH-EASY-ROESY experiments were

applied to the cyclic undecapeptide cyclosporine A, whose (*pure shift*) EASY-ROESY spectra are usually dominated by t_1-noise in the *N*-methyl region. For the *pure shift* experiments studied we could prove that the extracted proton-proton distances are accurate within the typical error ranges expected for NOE analysis, either by comparing them with expected values for proton pairs within rigid moieties and *a priori* known distances or by the comparison between interproton distances extracted from different types of ROESY experiments. We therefore expect that the presented methods will be valuable experiments in a wide range of structure elucidation applications, including the investigation of complex natural products, drugs or transition metal complexes.

7 Experimental section

Experiments on the tetrapeptide *R,R*-diol sample were performed on a Bruker Avance III HD spectrometer operating at 700.17 MHz proton base frequency equipped with a QCI probe (^{1}H/^{19}F ^{13}C/^{31}P, ^{15}N-D) with *z*-gradient (0.53 T m^{-1} maximum gradient strength). The sample temperature was 300 K. 2D *F*1-PSYCHE-EASY-ROESY spectra were acquired with the pulse sequence in chapter 8.1 of the SI. Mixing-times were 150 ms, 200 ms, 300 ms, 375 ms and 400 ms. 8 scans per t_1-increment with a recovery delay of 14 s were acquired.

Experiments with the cyclosporine A sample were done on a Bruker Avance III spectrometer with 600.3 MHz proton base frequency, equipped with a 5 mm triple-resonance broadband inverse probe (^{1}H, ^{31}P, BB-D) with *z*-gradient (0.494 T m^{-1} maximum gradient strength). Sample temperature was 300 K.

2D *gradient-selected F*1-PSYCHE-EASY-ROESY spectra were acquired with the pulse sequence in chapter 8.2 of the SI. Mixing-times were 50 ms, 100 ms, 200 ms, 300 ms, 400 ms and 500 ms. 8 scans per t_1-increment with a recovery delay of 7.5 s were acquired. 2D *gradient-selected F*1-*perfect*BASH-EASY-ROESY spectra were acquired with the pulse sequence in chapter 8.3 of the SI. Mixing-times were 50 ms, 100 ms, 125 ms, 150 ms, 200 ms and 250 ms. The spectral width in the indirect dimension *F*1 and the bandwidths of the selective refocusing pulses were set to cover the amide- and α-proton region of cyclosporine A. 8 scans per t_1-increment with a recovery delay of 7.5 s were acquired.

1D *gradient-selected* CW-ROESY and 1D *gradient-selected* EASY-ROESY spectra were acquired with the pulse sequences in chapter 8.4 and 8.5 of the SI. Mixing-times were 50 ms, 100 ms, 200 ms, 300 ms, 400 ms and 500 ms. For selective refocusing RSnob shaped pulses[93] with bandwidths appropriate to the selected proton were used. 32 or 64 scans per mixing-time with a recovery delay of 7.5 s were acquired.

Detailed experimental descriptions for all acquired ROESY spectra can be found in chapter 1 of the SI

8 Acknowledgements

J.I. acknowledges the funding with a PhD fellowship by the Studienstiftung des deutschen Volkes. J.N. and C.M.T thanks the Deutsche Forschungsgesellschaft (DFG) for funding (TH1115/12-1). We thank Dr. Jonas Kind and Dr. Davy Sinnaeve for helpful discussions.

9 References

[1] M. Karplus, Vicinal Proton Coupling in Nuclear Magnetic Resonance, J. Am. Chem. Soc., 85 (1963) 2870-2871.
[2] C. Altona, Vicinal Coupling Constants and Conformation of Biomolecules, in: eMagRes (eds R.K. Harris and R.L. Wasylishen), John Wiley, Chichester, 2007.
[3] P. E. Hansen, Carbon—hydrogen spin—spin coupling constants, Prog. Nucl. Magn. Reson. Spectrosc., 14 (1981) 175-295.
[4] W. A. Thomas, Unravelling molecular structure and conformation—the modern role of coupling constants, Prog. Nucl. Magn. Reson. Spectrosc., 30 (1997) 183-207.
[5] A. W. Overhauser, Polarization of Nuclei in Metals, Phys. Rev., 92 (1953) 411-415.
[6] I. Solomon, Relaxation Processes in a System of Two Spins, Phys. Rev., 99 (1955) 559-565.
[7] R. A. Bell, J. K. Saunders, Correlation of the intramolecular nuclear Overhauser effect with internuclear distance, Can. J. Chem., 48 (1970) 1114-1122.
[8] F. A. L. Anet, A. J. R. Bourn, Nuclear Magnetic Resonance Spectral Assignments from Nuclear Overhauser Effects1, J. Am. Chem. Soc., 87 (1965) 5250-5251.
[9] D. Neuhaus, M. P. Williamson, The nuclear Overhauser effect in structural and conformational analysis, Second Edition ed., Wiley-VCH, New York, 2000.
[10] A. A. Bothner-By, R. L. Stephens, J. Lee, C. D. Warren, R. W. Jeanloz, Structure determination of a tetrasaccharide: transient nuclear Overhauser effects in the rotating frame, J. Am. Chem. Soc., 106 (1984) 811-813.
[11] A. Bax, D. G. Davis, Practical Aspects of Two-Dimensional Transverse NOE Spectroscopy, J. Magn. Reson., 63 (1985) 207-213.
[12] A. Bax, S. Grzesiek, ROESY, in: eMagRes (eds R.K. Harris and R.L. Wasylishen), John Wiley, Chichester, 2007.
[13] C. Griesinger, R. R. Ernst, Frequency offset effects and their elimination in NMR rotating-frame cross-relaxation spectroscopy, J. Magn. Reson., 75 (1987) 261-271.
[14] H. Kessler, C. Griesinger, R. Kerssebaum, K. Wagner, R. R. Ernst, Separation of cross-relaxation and J cross-peaks in 2D rotating-frame NMR spectroscopy, J. Am. Chem. Soc., 109 (1987) 607-609.
[15] A. Bax, Correction of cross-peak intensities in 2D spin-locked NOE spectroscopy for offset and Hartmann-Hahn effects, J. Magn. Reson., 77 (1988) 134-147.
[16] J. Cavanagh, J. Keeler, Suppression of HOHAHA and “false” NOE cross peaks in CAMELSPIN spectra, J. Magn. Reson., 80 (1988) 186-194.
[17] T. L. Hwang, A. J. Shaka, Cross Relaxation without TOCSY - Transverse Rotating-Frame Overhauser Effect Spectroscopy, J. Am. Chem. Soc., 114 (1992) 3157-3159.
[18] T.-L. Hwang, M. Kadkhodaei, A. Mohebbi, A. J. Shaka, Coherent and incoherent magnetization transfer in the rotating frame, Magn. Reson. Chem., 30 (1992) S24-S34.
[19] J. Schleucher, J. Quant, S. J. Glaser, C. Griesinger, A Theorem Relating Cross-Relaxation and Hartmann-Hahn Transfer in Multiple-Pulse Sequences - Optimal Suppression of TOCSY Transfer in ROESY, J. Magn. Reson., 112 (1995) 144-151.
[20] J. Schleucher, J. Quant, S. J. Glaser, C. Griesinger, TOCSY in ROESY and ROESY in TOCSY, in: eMagRes (eds R.K. Harris and R.L. Wasylishen), John Wiley, Chichester, 2007.
[21] C. M. Thiele, K. Petzold, J. Schleucher, EASY ROESY: reliable cross-peak integration in adiabatic symmetrized ROESY, Chem. Eur. J., 15 (2009) 585-588.
[22] R. W. Adams, Pure Shift NMR Spectroscopy, eMagRes, 3 (2014) 295–310.
[23] K. Zangger, Pure shift NMR, Prog. Nucl. Magn. Reson. Spectrosc., 86-87 (2015) 1-20.

[24] L. Castañar, T. Parella, Broadband 1H homodecoupled NMR experiments: recent developments, methods and applications, Magn. Reson. Chem., 53 (2015) 399-426.
[25] L. Castañar, Pure shift 1 H NMR: what is next?, Magn. Reson. Chem., 55 (2017) 47-53.
[26] M. J. Thrippleton, J. Keeler, Elimination of zero-quantum interference in two-dimensional NMR spectra, Angew. Chem. Int. Ed., 42 (2003) 3938-3941.
[27] S. Boros, G. Batta, Offset-compensated and zero-quantum suppressed ROESY provides accurate 1 H-1 H distances in small to medium-sized molecules, Magn. Reson. Chem., 54 (2016) 947-952.
[28] L. Castañar, P. Nolis, A. Virgili, T. Parella, Measurement of T_1/T_2 relaxation times in overlapped regions from homodecoupled ^{1}H singlet signals, J. Magn. Reson., 244 (2014) 30-35.
[29] V. M. Rao Kakita, V. K. Shukla, M. Bopardikar, T. Bhattacharya, Ramakrishna V. Hosur, Measurement of 1H NMR relaxation times in complex organic chemical systems: application of PSYCHE, RSC Advances, 6 (2016) 100098-100102.
[30] L. Kaltschnee, A. Kolmer, I. Timári, V. Schmidts, R. W. Adams, M. Nilsson, K. E. Kövér, G. A. Morris, C. M. Thiele, "Perfecting" pure shift HSQC: full homodecoupling for accurate and precise determination of heteronuclear couplings, Chem. Commun., 50 (2014) 15702-15705.
[31] I. Timári, L. Kaltschnee, A. Kolmer, R. W. Adams, M. Nilsson, C. M. Thiele, G. A. Morris, K. E. Kövér, Accurate determination of one-bond heteronuclear coupling constants with "pure shift" broadband proton-decoupled CLIP/CLAP-HSQC experiments, J. Magn. Reson., 239 (2014) 130-138.
[32] I. Timári, T. Z. Illyes, R. W. Adams, M. Nilsson, L. Szilagyi, G. A. Morris, K. E. Kövér, Precise measurement of long-range heteronuclear coupling constants by a novel broadband proton-proton-decoupled CPMG-HSQMBC method, Chem. Eur. J., 21 (2015) 3472-3479.
[33] I. Timári, L. Szilagyi, K. E. Kövér, PSYCHE CPMG-HSQMBC: An NMR Spectroscopic Method for Precise and Simple Measurement of Long-Range Heteronuclear Coupling Constants, Chem. Eur. J., 21 (2015) 13939-13942.
[34] T. Reinsperger, B. Luy, Homonuclear BIRD-decoupled spectra for measuring one-bond couplings with highest resolution: CLIP/CLAP-RESET and constant-time-CLIP/CLAP-RESET, J. Magn. Reson., 239 (2014) 110-120.
[35] A. J. Pell, J. Keeler, Two-dimensional J-spectra with absorption-mode lineshapes, J. Magn. Reson., 189 (2007) 293-299.
[36] M. Foroozandeh, R. W. Adams, P. Király, M. Nilsson, G. A. Morris, Measuring couplings in crowded NMR spectra: pure shift NMR with multiplet analysis, Chem. Commun., 51 (2015) 15410-15413.
[37] D. Sinnaeve, M. Foroozandeh, M. Nilsson, G. A. Morris, A General Method for Extracting Individual Coupling Constants from Crowded ^{1}H NMR Spectra, Angew. Chem. Int. Ed., 55 (2016) 1090-1093.
[38] A. Cotte, D. Jeannerat, 1D NMR Homodecoupled ^{1}H Spectra with Scalar Coupling Constants from 2D NemoZS-DIAG Experiments, Angew. Chem. Int. Ed., 54 (2015) 6016-6018.
[39] N. Marco, A. A. Souza, P. Nolis, R. R. Gil, T. Parella, Perfect 1JCH-resolved HSQC: Efficient measurement of one-bond proton-carbon coupling constants along the indirect dimension, J. Magn. Reson., 276 (2017) 37-42.
[40] J. Ying, J. Roche, A. Bax, Homonuclear decoupling for enhancing resolution and sensitivity in NOE and RDC measurements of peptides and proteins, J. Magn. Reson., 241 (2014) 97-102.
[41] L. Castañar, M. Garcia, E. Hellemann, P. Nolis, R. R. Gil, T. Parella, One-Shot Determination of Residual Dipolar Couplings: Application to the Structural Discrimination of Small Molecules Containing Multiple Stereocenters, J. Org. Chem., 81 (2016) 11126-11131.
[42] D. Sinnaeve, J. Ilgen, M. E. Di Pietro, J. J. Primozic, V. Schmidts, C. M. Thiele, B. Luy, Probing Long-Range Anisotropic Interactions: a General and Sign-Sensitive Strategy to Measure ^{1}H-^{1}H Residual Dipolar Couplings as a Key Advance for Organic Structure Determination, Angew. Chem. Int. Ed., 59 (2020) 5316-5320.
[43] G. Aloui, S. Bouabdallah, J. P. Baltaze, J. E. H. Pucheta, S. Touil, J. Farjon, N. Giraud, Monitoring Conformational Changes in an Enzyme Conversion Inhibitor Using Pure Shift Exchange NMR Spectroscopy, ChemPhysChem, 20 (2019) 1738-1746.
[44] J. M. McKenna, J. A. Parkinson, HOBS methods for enhancing resolution and sensitivity in small DNA oligonucleotide NMR studies, Magn. Reson. Chem., 53 (2015) 249-255.

[45] L. Kaltschnee, K. Knoll, V. Schmidts, R. W. Adams, M. Nilsson, G. A. Morris, C. M. Thiele, Extraction of distance restraints from pure shift NOE experiments, J. Magn. Reson., 271 (2016) 99-109.
[46] M. Foroozandeh, R. W. Adams, N. J. Meharry, D. Jeannerat, M. Nilsson, G. A. Morris, Ultrahigh-resolution NMR spectroscopy, Angew. Chem. Int. Ed., 53 (2014) 6990-6992.
[47] J. Ilgen, L. Kaltschnee, C. M. Thiele, perfectBASH: Band-selective homonuclear decoupling in peptides and peptidomimetics, Magn. Reson. Chem., 56 (2018) 918-933.
[48] C. E. Müller, L. Wanka, K. Jewell, P. R. Schreiner, Enantioselektive kinetische Racematspaltung von trans-Cycloalkan-1,2-diolen, Angew. Chem., 120 (2008) 6275-6278.
[49] E. Procházková, A. Kolmer, J. Ilgen, M. Schwab, L. Kaltschnee, M. Fredersdorf, V. Schmidts, R. C. Wende, P. R. Schreiner, C. M. Thiele, Uncovering Key Structural Features of an Enantioselective Peptide-Catalyzed Acylation Utilizing Advanced NMR Techniques, Angew. Chem. Int. Ed., 55 (2016) 15754-15759.
[50] C. Dalvit, Semi-selective two-dimensional homonuclear and heteronuclear NMR experiments recorded with pulsed field gradients, Magn. Reson. Chem., 33 (1995) 570-576.
[51] T. Parella, F. Sánchez-Ferrando, A. Virgili, Quick Recording of Pure Absorption 2D TOCSY, ROESY, and NOESY Spectra Using Pulsed Field Gradients, J. Magn. Reson., 125 (1997) 145-148.
[52] J. A. Aguilar, A. A. Colbourne, J. Cassani, M. Nilsson, G. A. Morris, Decoupling two-dimensional NMR spectroscopy in both dimensions: pure shift NOESY and COSY, Angew. Chem. Int. Ed., 51 (2012) 6460-6463.
[53] R. Brüschweiler, C. Griesinger, O. W. Sørensen, R. R. Ernst, Combined use of hard and soft pulses for ω1 decoupling in two-dimensional NMR spectroscopy, J. Magn. Reson., 78 (1988) 178-185.
[54] V. M. Kakita, J. Bharatam, Real-time homonuclear broadband and band-selective decoupled pure-shift ROESY, Magn. Reson. Chem., 52 (2014) 389-394.
[55] A. Kaerner, D. L. Rabenstein, An ω1-band-selective, ω1-homonuclear decoupled ROESY experiment: application to the assignment of 1H NMR spectra of difficult-to-assign peptide sequences, Magn. Reson. Chem., 36 (1998) 601-607.
[56] L. Castañar, P. Nolis, A. Virgili, T. Parella, Full sensitivity and enhanced resolution in homodecoupled band-selective NMR experiments, Chem. Eur. J., 19 (2013) 17283-17286.
[57] J. R. Garbow, D. P. Weitekamp, A. Pines, Bilinear Rotation Decoupling of Homonuclear Scalar Interactions, Chem. Phys. Lett., 93 (1982) 504-509.
[58] K. Zangger, H. Sterk, Homonuclear broadband-decoupled NMR spectra, J. Magn. Reson., 124 (1997) 486-489.
[59] M. Foroozandeh, R. W. Adams, M. Nilsson, G. A. Morris, Ultrahigh-resolution total correlation NMR spectroscopy, J. Am. Chem. Soc., 136 (2014) 11867-11869.
[60] M. Foroozandeh, L. Castañar, L. G. Martins, D. Sinnaeve, G. D. Poggetto, C. F. Tormena, R. W. Adams, G. A. Morris, M. Nilsson, Ultrahigh-Resolution Diffusion-Ordered Spectroscopy, Angew. Chem. Int. Ed., 55 (2016) 15579-15582.
[61] M. Foroozandeh, G. A. Morris, M. Nilsson, PSYCHE Pure Shift NMR Spectroscopy, Chem. Eur. J., 24 (2018) 13988-14000.
[62] A. Lupulescu, G. L. Olsen, L. Frydman, Toward single-shot pure-shift solution 1H NMR by trains of BIRD-based homonuclear decoupling, J. Magn. Reson., 218 (2012) 141-146.
[63] N. H. Meyer, K. Zangger, Simplifying proton NMR spectra by instant homonuclear broadband decoupling, Angew. Chem. Int. Ed., 52 (2013) 7143-7146.
[64] A. F. Mehlkopf, D. Korbee, T. A. Tiggelman, R. Freeman, Sources of t1 noise in two-dimensional NMR, J. Magn. Reson., 58 (1984) 315-323.
[65] G. A. Morris, Systematic sources of signal irreproducibility and t1 noise in high-field NMR spectrometers, J. Magn. Reson., 100 (1992) 316-328.
[66] J. Stonehouse, P. Adell, J. Keeler, A. J. Shaka, Ultrahigh-Quality NOE Spectra, J. Am. Chem. Soc., 116 (1994) 6037-6038.
[67] D. Marion, M. Ikura, R. Tschudin, A. Bax, Rapid recording of 2D NMR spectra without phase cycling. Application to the study of hydrogen exchange in proteins, J. Magn. Reson., 85 (1989) 393-399.
[68] J. Ilgen, L. Kaltschnee, C. M. Thiele, A pure shift experiment with increased sensitivity and superior performance for strongly coupled systems, J. Magn. Reson., 286 (2018) 18-29.

[69] G. Otting, L. P. M. Orbons, K. Wüthrich, Suppression of Zero-Quantum Coherence in NOESY and Soft NOESY, J. Magn. Reson., 89 (1990) 423-430.
[70] A. Hammarström, G. Otting, Improved Spectral Resolution in 1H NMR Spectroscopy by Homonuclear Semiselective Shaped Pulse Decoupling during Acquisition, J. Am. Chem. Soc., 116 (1994) 8847-8848.
[71] J. Wang, D. Borchardt, D. L. Rabenstein, Improved resolution in two-dimensional 1H NMR spectra of peptides by band-selective, homonuclear decoupling during both the evolution and acquisition periods: application to characterization of the binding of peptides by heparin, Magn. Reson. Chem., 44 (2006) 744-752.
[72] V. V. Krishnamurthy, Application of Semi-Selective Excitation Sculpting for Homonuclear Decoupling During Evolution in Multi-Dimensional NMR, Magn. Reson. Chem., 35 (1997) 9-12.
[73] W.-L. Chuang, M. D. Christ, D. L. Rabenstein, Determination of the Primary Structures of Heparin- and Heparan Sulfate-Derived Oligosaccharides Using Band-Selective Homonuclear-Decoupled Two-Dimensional 1H NMR Experiments, Anal. Chem., 73 (2001) 2310-2316.
[74] K. Takegoshi, K. Ogura, K. Hikichi, A perfect spin echo in a weakly homonuclear J-coupled two spin- system, J. Magn. Reson., 84 (1989) 611-615.
[75] P. C. M. van Zijl, C. T. W. Moonen, M. von Kienlin, Homonuclear J refocusing in echo spectroscopy, J. Magn. Reson., 89 (1990) 28-40.
[76] A. Verma, S. Bhattacharya, B. Baishya, Perfecting band selective homo-decoupling for decoupling two signals coupled within the same band, RSC Advances, 8 (2018) 19990-19999.
[77] M. R. Koos, G. Kummerlöwe, L. Kaltschnee, C. M. Thiele, B. Luy, CLIP-COSY: A Clean In-Phase Experiment for the Rapid Acquisition of COSY-type Correlations, Angew. Chem. Int. Ed., 55 (2016) 7655-7659.
[78] C. P. Butts, C. R. Jones, E. C. Towers, J. L. Flynn, L. Appleby, N. J. Barron, Interproton distance determinations by NOE – surprising accuracy and precision in a rigid organic molecule, Org. Biomol. Chem., 9 (2011) 177-184.
[79] S. Macura, B. T. Farmer, L. R. Brown, An improved method for the determination of cross-relaxation rates from NOE data, J. Magn. Reson., 70 (1986) 493-499.
[80] H. Hu, K. Krishnamurthy, Revisiting the initial rate approximation in kinetic NOE measurements, J. Magn. Reson., 182 (2006) 173-177.
[81] G. H. Weiss, J. A. Ferretti, J. E. Kiefer, L. Jacobson, A method for eliminating error due to phase imperfection in NOE measurements, J. Magn. Reson., 53 (1983) 7-13.
[82] G. H. Weiss, J. A. Ferretti, Accuracy and precision in the estimation of peak areas and NOE factors, J. Magn. Reson., 55 (1983) 397-407.
[83] J. A. Ferretti, A. K. Weiss, G. H. Weiss, Errors in the measurement of NOE factors, J. Magn. Reson., 62 (1985) 319-321.
[84] G. H. Weiss, J. E. Kiefer, J. A. Ferretti, Accuracy and precision in the estimation of internuclear distances for structure determinations, J. Magn. Reson., 97 (1992) 227-234.
[85] T. A. Halgren, Merck molecular force field. V. Extension of MMFF94 using experimental data, additional computational data, and empirical rules, J. Comput. Chem., 17 (1996) 616-641.
[86] K. F. Sheberstov, E. Sistaré Guardiola, M. Pupier, D. Jeannerat, SAN plot: A graphical representation of the signal, noise, and artifacts content of spectra, Magn. Reson. Chem., n/a (2019).
[87] H. Kessler, H. R. Loosli, H. Oschkinat, Peptide conformations. Part 30. Assignment of the 1H-, 13C-, and 15N-NMR spectra of cyclosporin A in CDCl3 and C6D6 by a combination of homo- and heteronuclear two-dimensional techniques, Helvetica Chimica Acta, 68 (1985) 661-681.
[88] H. R. Loosli, H. Kessler, H. Oschkinat, H. P. Weber, J. Petcher Trevor, A. Widmer, Peptide conformations. Part 31. The conformation of cyclosporin a in the crystal and in solution, Helvetica Chimica Acta, 68 (1985) 682-704.
[89] J. Klages, C. Neubauer, M. Coles, H. Kessler, B. Luy, Structure Refinement of Cyclosporin A in Chloroform by Using RDCs Measured in a Stretched PDMS-Gel, ChemBioChem, 6 (2005) 1672-1678.
[90] S. Efimov, Y. Zgadzay, V. Klochkov, Observation of Conformational Exchange in Cyclosporin in Media of Varying Polarity by NMR Spectroscopy, Appl. Magn. Reson., 45 (2014) 1225-1235.
[91] S. V. Efimov, F. K. Karataeva, A. V. Aganov, S. Berger, V. V. Klochkov, Spatial structure of cyclosporin A and insight into its flexibility, J. Mol. Struct., 1036 (2013) 298-304.

[92] J. W. Keepers, T. L. James, A theoretical study of distance determinations from NMR. Two-dimensional nuclear overhauser effect spectra, J. Magn. Reson., 57 (1984) 404-426.
[93] E. Kupče, J. Boyd, I. D. Campbell, Short selective pulses for biochemical applications, J. Magn. Reson., 106 (1995) 300-303.